EFFECT OF NON-METAL ELEMENTS (C, N, S) AS ANIONIC DOPANTS ON ELECTRONIC STRUCTURE OF TiO_2-ANATASE BY DENSITY-FUNCTIONAL THEORY APPROACH

PENGARUH UNSUR-UNSUR NON-LOGAM (C, N, S) SEBAGAI PENDADAH ANIONIK TERHADAP STRUKTUR ELEKTRONIK TiO_2-ANATAS DENGAN PENDEKATAN *DENSITY FUNCTIONAL THEORY*

Hari Sutrisno

Department of Chemistry Education, Faculty of Mathematics and Natural Sciences, Yogyakarta State University, Yogyakarta, Indonesia

email: sutrisnohari@uny.ac.id

Received 9 February 2016; Accepted 4 April 2016; Available online 16 May 2016

ABSTRACT

This article is a theoritical approach to calculate the electronic structure of undoped- and non-metal anions doped-TiO_2-anatase. The objective of the research is to calculate ab-initio the band structure and the density of states (DOS) of undoped-, C-, N-, and S-doped TiO_2-anatase. Kohn-Sham equations are performed with the density functional theory (DFT) using the local density approximation (LDA) for exchange-correlation functional. The first-principle calculations were done using supercell (2x2x1) methods as implemented within Amsterdam Density Functional (ADF)-BAND version 2014.10. The ab-initio calculation of the band structures show that all samples are direct- and indirect-gap type semiconductor. The band gap of TiO_2-anatase with DFT using LDA is 2.43 eV. The addition of C atom at 0.943% in 48 atoms produces width intermediate band about 0.76 eV, which is 0.38 eV above the valence band (VB) and 1.38 eV below the conduction band (CB). The addition of N atom at 1.103% and S atom at 2.478% in the lattice structure of TiO_2-anatase resulted in the addition of the VB width to 0.47 eV and 0.11 eV, while the resulting gap between the VB and the CB to 1.97 eV and 2.33 eV, respectively.

Keywords: anatase, band gap, density-functional theory, electronic structure, first-principle calculation

ABSTRAK

Artikel ini merupakan kajian teoritik struktur pita dan *density of states* (DOS) dalam TiO_2-anatas dan TiO_2-anatas terdadah anion non-logam. Tujuan penelitian yaitu menghitung secara *ab-initio* energi celah pita dan DOS dalam TiO_2-anatas dan TiO_2-anatas terdadah: -karbon (C-TiO_2), -nitrogen (N-TiO_2), dan -belerang (S-TiO_2). Persamaan Kohn-Sham digunakan untuk perhitungan prinsip awal secara *ab-initio* berdasarkan pendekatan *density-functional theory* (DFT) dan *local density approximation* (LDA) sebagai fungsi perubahan korelasi. Program Amsterdam Density Functional (ADF)-BAND versi 2014.10 digunakan untuk perhitungan awal dengan metode supersel (2x2x1). Hasil perghitungan menunjukkan TiO_2-anatas, C-TiO_2, N-TiO_2, dan S-TiO_2 merupakan tipe semikonduktor celah langsung (*direct-gap*) dan celah tidak langsung (*indirect-gap*). TiO_2-anatas memiliki energi celah pita minimum = 2,43 eV. Penambahan 0,943% C dalam 48 atom mengakibatkan lebar pita antara = 0,76 eV, terletak 0,38 eV di atas pita valensi dan 1,38 eV di bawah pita konduksi. Penambahan masing-masing 1,103% N dan 2,478% S dalam

TiO_2-anatas mengakibatkan pelebaran pita valensi berturut-turut sebesar 0,47 eV dan 0,11 eV, sedangkan jarak pita valensi dengan pita konduksi sebesar 1,97 eV dan 2,33 eV.

Kata kunci: anatase, celah pita, *density functional theory*, perhitungan prinsip awal, struktur elektronik,

INTRODUCTION

Titanium dioxide or titania (TiO_2) has been extensively studied in the past few years for being extremely useful in many applications. TiO_2 as a n-type semiconductor with a wide energy band gap, is well-known for potential applications due to their high photosensitivity, non-toxicity and low cost. TiO_2 has eleven polymorphs, but in nature, there are three kinds of crystal structure: anatase, rutile and brookite (Carp, Huisman, & Reller, 2004). Rutile is a stable phase, while anatase and brookite are metastable and will be transformed into a thermodynamically most stable rutile phase at higher temperature after thermal treatment. Anatase and rutile are both produced on an industrial scale. Anatase phase is a TiO_2 polymorph which is less stable than rutile phase, but more efficient than rutile for several applications, including photocatalysis (Muctuma, Shao, Kim, & Kim, 2015; Zhang et al., 2016), antibacterial activity (Galkina et al., 2014; Joost et al., 2015), dye sensitized solar cells (Chen, Hsu, Chan, Zhang, & Huang, 2014; Yang, Bark, Kim, & Choi, 2014) and sensor (Goyal, Kaur, & Pandey, 2010; Pustelny et al., 2012).

In all these applications, the surface properties of TiO_2 are of major importance in particular of the band gap energy. However, such potential applications are seriously limited by the intrinsic wide energy gaps of TiO_2, which confine the advantages of the TiO_2 phases to be viable only under UV radiation. If a wide-band gap semiconductor like titanium dioxide (TiO_2) is irradiated with light, excited electron–hole pairs result. When a photon of energy higher or equal to the band gap value of the semiconductor is absorbed by a particle, an electron from the valence band (VB) is promoted to the conduction band (CB) with simultaneous generation of a photogenerated hole (h_{vb}^+) in the VB and photogenerated electron (e_{cb}^-) in the CB. The rutile phase, which is the most stable form of TiO_2, exhibits a direct band gap of 3.0 eV, while the band gap of the metastable anatase phase is indirect band structure of 3.2 eV and the band gap of the metastable brookite is 3,4 eV (Persson & Ferreira da Silva, 2005; Tian-Hua, Chen-Lu, Yong, & Gao-Rong, 2006).

Many attempts have been reduced the band gaps energy to improve the photoactivity performance of TiO_2 under visible-light irradiation. A number of methods have been studied to decrease the band gap energy of TiO_2. The most promising method to reduce the effective band gap of TiO_2 is through the doping of impurities into the TiO_2 lattice through substitual or interstitial to modify its electronic structure. Especially in recent years, a number of attempts have been made to improve the visible-light absorption of TiO_2 both with transition metal: V, Mn, Fe, Cu, Ce, Cr, Ag, etc. (Al-Hartomy, 2014; Chang & Liu, 2014; Liu et al., 2009; Tian, Li & Zhang, 2012; Wang, Zang, Li, Li, & Lin, 2014; Zhang, Liu, Han, & Piao, 2013) and non-metal: B, C, N, S, F, etc. (Asahi, Morikawa, Ohwaki, Aoki, & Taga, 2001; Dong, Zhao, & Wu, 2008; Zhao, Wu, Tang & Jiang, 2013), to modify the electronic structure and improve the photocatalytic reaction efficiency which strongly influenced by the recombination rate of photo-generated electrons and holes.

Various non-metal as dopants substituted into the structure of TiO_2 has been extensively studied experimentally and theoretical calculations performed to shift the TiO_2 absorption of ultra- violet

region to the visible region. Anion non-metal as dopants, such as boron (B), carbon (C) , nitrogen (N) , and sulfur (S) (Asahi et al., 2001; Dong et al., 2008; Tian-Hua et al., 2006; Zhao et al., 2013; Zhao, Qiu, & Burda, 2008; Yang et al., 2007), has made it known to have photocatalytic performance in visible region The objective of the research is to calculate the electronic structure consisting of the band structure and the density of states (DOS) of material such as TiO_2-anatase, C-, N-, and S-doped TiO_2-anatase based on density functional theory (DFT) approach. The anions of C^{4-} , N^{3-} , and S^{2-} as dopants substitute into the lattice structure of TiO_2-anatase through the replacement of anions O^{2-} to modify the electronic structure. The (2×2×1) supercell model of C-, N-, or S-doped TiO_2-anatase phase contains 48 atoms, in this way the structure of $Ti_{16}O_{31}X$ (X = C, N, or S) are obtained and the percentage of dopant atoms theoretically are found to be at 0.943% atom C, 1.103% atom N and 2.478% atom S. Based on the theoretical information of the band structure and the density of states (DOS), it will be known systematically the influence anionic non-metallic atoms on the band gap minimum and very helpful in the selection of photocatalyst.

CALCULATION AND EXPERIMENTAL METHODS

Hardware and Software

The first-principle calculations were done by using hardware PC (personal computer) with specifications: Processor Intel (R) Core (TM) 2 Duo CPU T8100 @ 2,10 GHz, hard disk 230 GB, RAM 3 GB and display card (VGA) 1.5 GB. The density function theory (DFT) calculations of materials were performed on the operating system Windows Vista™ Premium Edition Familial. The electronic properties of all materials have been investigated using Amsterdam Density Functional (ADF) package of ADF-BAND version 2014.10 (Team SCM, 2014).

Computational Method and Details

All calculations presented are based on density-functional theory (DFT) approach. The Kohn-Sham equation calculations are performed with the density functional theory (DFT) using the local density approximation (LDA) (Kohn & Sham, 1965) for the exchange-correlation functional. The first-principle calculations were done using supercell (2x2x1) method. The cell of TiO_2-anatase, C-, N-, and S-doped TiO_2-anatase in a (2x2x1) supercell model considered in this study are shown in **Figure 1**. The ideal anatase TiO_2 has a tetragonal structure with space group $I4_1/amd$, which contains four titanium atoms and eight oxygen atoms in unit cell. The cell parameters are a = b = 3,8048 Å and c = 9,5962 Å (Sutrisno, 2012).

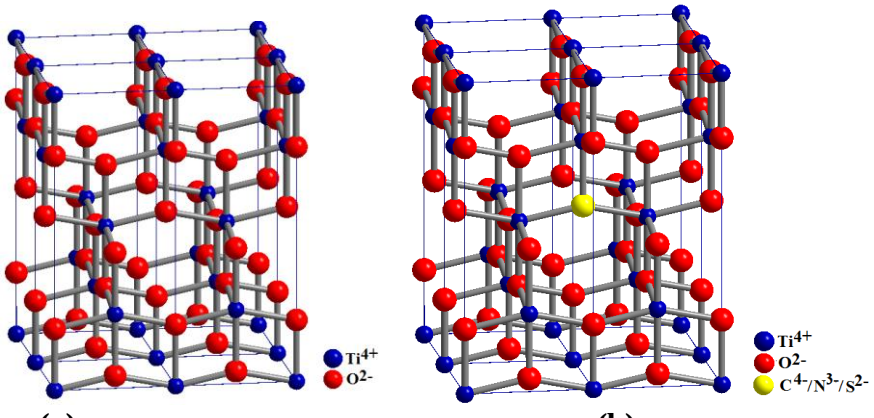

(a) **(b)**

Figure 1. Structure of (2x2x1) supercell model containing 48 atoms of (a). TiO_2-anatase and (b). C-, N-, or S-doped TiO_2-anatase

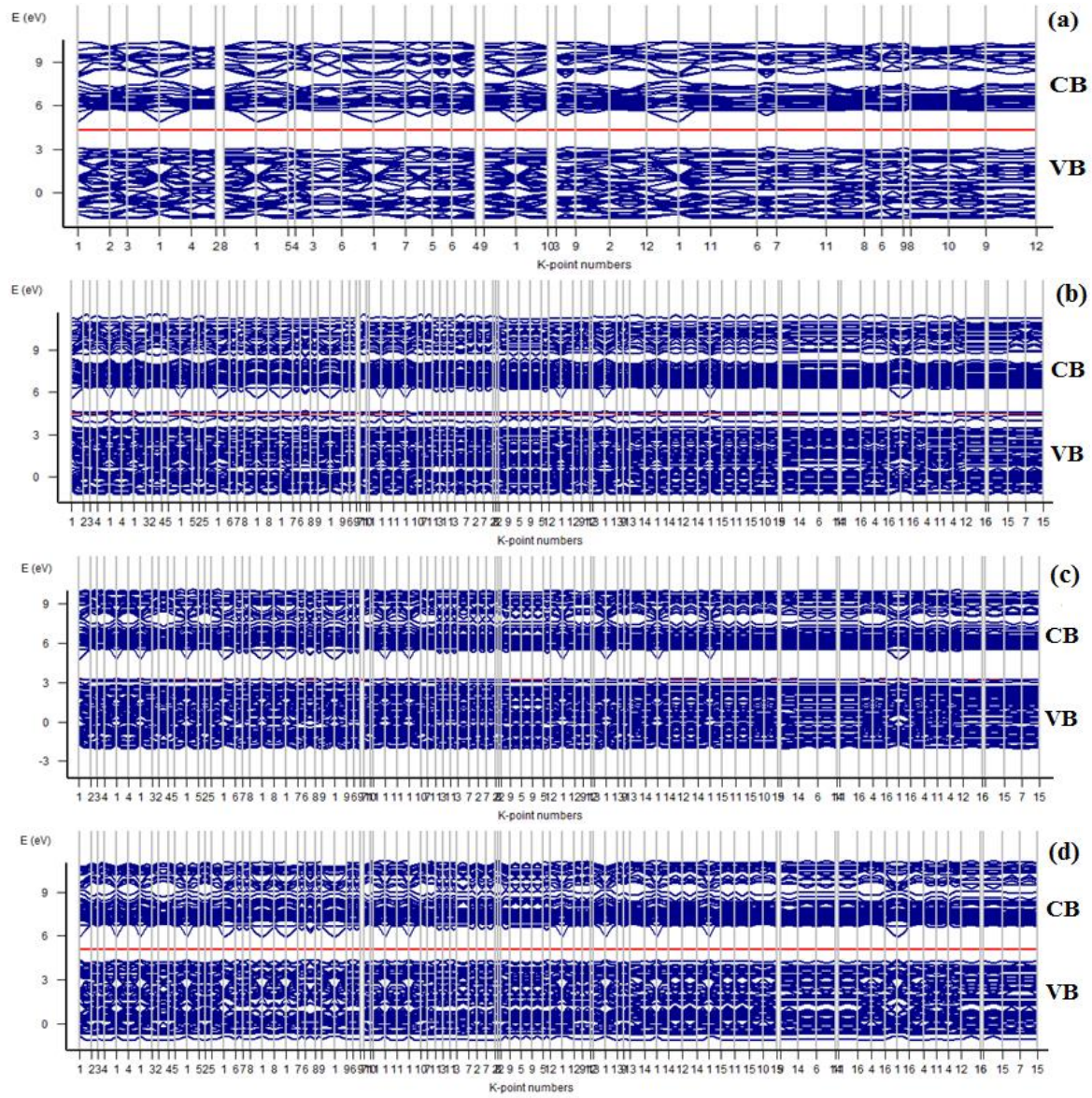

Figure 2. Band structures of (a). TiO_2-anatase, (b). C-doped TiO_2-anatase, (c). N-doped TiO_2-anatase, and (d). S-doped TiO_2-anatase

In C-, N-, and S-doped TiO_2-anatase, an O^{2-} ion is replaced by one C^{4-}, N^{3-}, or S^{2-} ion, respectively. For C-, N- or S-doped TiO_2-anatase (**Figure 3b-3d**), it is clear that: some C 2*p*, N 2*p* or S 2*p* states is hybridized with O 2*p* states in the valence band, while other C 2*p*, N 2*p* or S 2*p* states localized on the top valence band maximum (VBM) as acceptor level.

The calculated t-DOS and p- DOS of C doped TiO_2-anatase containing C atom at 0.943% are shown in **Figure 3b**. The t-DOS characters of C-doped TiO_2-anatase show that the valence band is mainly composed of O 2*p* states and C 2*p*, while the conduction band of the contribution of Ti 3*d* states.

In **Figure 3b** show the existence of four groups: the area around -14 eV to -12 eV is mainly composed of O 2*s* states, the area around -4 eV is the 2*s* states of C, the area around -1 eV to 3.5 eV (VB) located below the Fermi Energy (E_F) mainly consists of O 2*p* state , the area around 4 eV to 5 eV is mainly composed of C 2*p* states, and the area around 5 eV to 11 eV (CB) located above the Fermi Energy mainly consists of Ti 3*d* states. As a result of the presence of intermediate band created two forms of band gap is 0.38 eV and 1.38 eV.

The addition of N^{3-} ions at 1.103% and S^{2-} ions at 2.478% in the lattice structure of TiO_2-anatase by substitution of O^{2-} ions create the same DOS character and is able to widen the valence band. The addition of N ions were able to widen the valence band of 0.47 eV, while the S ions were able to widen the valence band of 0.11 eV. The character t-DOS of N-doped TiO_2-anatase show that the valence band is mainly composed of O 2*p* states and N 2*p*, while the main contribution in the conduction band is derived from the 3d states of Ti.

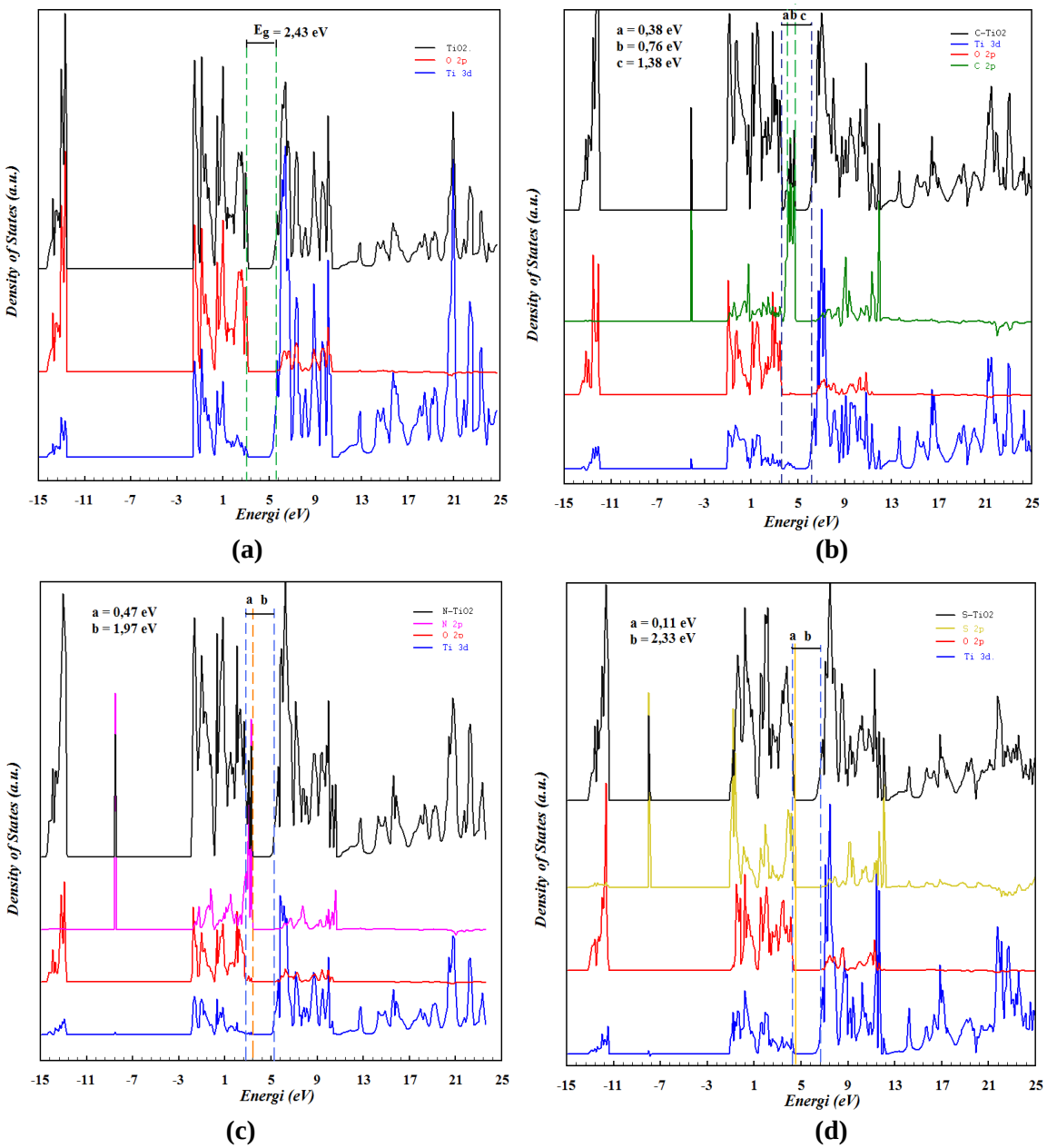

Figure 3. The total- and partial-Density of States (DOS) of (a). TiO_2-anatase, (b). C-doped TiO_2-anatase, (c). N-doped TiO_2-anatase, and (d). S-doped TiO_2-anatase

In **Figure 3c** , it appears there are three main groups: the area around -14.5 eV to -13 eV is the 2s states of O, the area around -8.5 eV is the 2s states of N, the area around -2 eV to 3.3 eV (VB) located below the Fermi energy (E_F) mainly consists of the 2p states of O and the 2p states of N, and the area around 5 eV to 10.5 eV (CB) located above the Fermi energy mainly consists of the 3d ststes of Ti. The N 2*p* states is hybridized with O 2*p* states and localized on the valence band maximum. This phenomenon matches the results of research from Asahi et al. (2001). The addition of the valence band of 0.47 eV due to the presence of N^{3-} ions increase the width of the valence band becomes 5.27 eV and led to the formation of intermediate band which is located between the valence band and the conduction band of 1.97 eV. The energy band gap calculation of N-doped TiO_2-anatase has a lower energy than the band gap energy of the measurement results (2.33 eV) (Zhao et al., 2013).

The t-DOS characters of S-doped TiO_2-anatase show that the valence band primarily consists of the O 2*p* states and S 2*p* states, while the conduction band mainly composed of Ti 3*d* states.

In **Figure 3d**, it appears there are four main groups: the area around -13 eV to -12 eV mainly consists of O 2s states, the area around -8 eV is the 2s states of S, the area around -1 eV to 4.3 eV (VB) located below the Fermi >Energy (E_F) is primarily composed of O 2*p* states and S 2*p* states, and the area around 6 eV to 12 eV (CB) located above the Fermi Energy mainly consists of Ti 3*d* states. The addition of the valence band width due to the presence of S^{2-} ion is 0.11eV, so that the width of the valence band to 5.41 eV and created a gap between the valence band and the conduction band to 2.33 eV.

Based on the above explanation, it can be concluded that the addition of dopants atom non-metal: C, N, and S into the lattice structure of TiO_2-anatase through the substitution of O atoms result in two types of changes in the band structure of TiO_2-anatase (**Figure 1**).

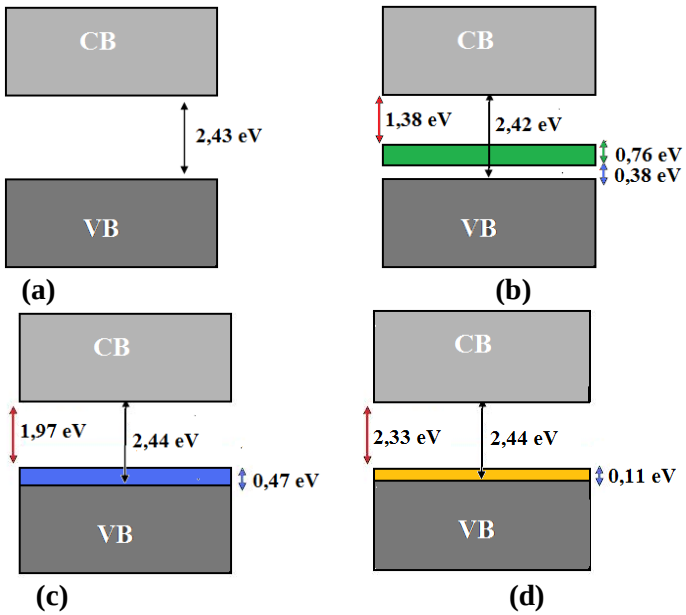

Figure 4. (a). The band gap of TiO_2-anatase, (b). the band structure of C-doped TiO_2-anatase with intermediate band of C localized on the valence band maximum, (c) the band structure N-doped TiO_2-anatase with a reduction the band gap due to the widening of the valence band, and (d). the structure band of N-doped TiO_2-anatase with a reduction the band gap due to the widening of the valence band.

TiO_2-anatase with the level of dopants localized on the top valence band maximum, and (2). the reduction of the band gap due to the widening of the valence band. The addition of dopants atom C resulted in the formation of the intermediate band is localized on the valence band maximum, while the addition of dopants atoms N and S resulted in the reduction of the band gap due to the widening of the valence band (**Figure 4**).

CONCLUSION

The electronic structures of TiO_2-anatase, C-, N-, and S-doped TiO_2-anatase have been successfully calculated by first principles calculations using density funtional theory approach and local density approximation (LDA) as exchange-correlation functional with supercell (2x2x1) method. The calculated band structures indicate that TiO_2-anatase, C-, N-, and S-doped TiO_2-anatase are direct- and indirect-gap type semiconductors. The calculated minimum band gap of TiO_2-anatase is about 2.43 eV. The addition of C atom at 0.943% in 48 atoms produces width intermediate band about 0.76 eV, which is 0.38 eV above the valence band and 1.38 eV below the conduction band. Meanwhile, the addition of N atom at 1.103% and S atom at 2.478% in the lattice structure of TiO_2-anatase show the same phenomenon which can widen the valence band, thus reduce of the gap between the valence band and the conduction band. The calculated band gap of N-doped TiO_2-anatase resulted in the addition of the valence band width to 0.47 eV and the resulting gap between the valence band and the conduction band to 1.97 eV, while the calculation of the S-doped TiO_2-anatase resulted in the addition of the valence band width of 0.11 eV and the distance between the valence band and the conduction band to 2.33 eV.

REFERENCES

Al-Hartomy, O. A. (2014). Synthesis, characterization, photocatalytic and photovoltaic performance of Ag-doped TiO_2 load on the Pt-carbon spheres. *Materials Science in Semiconductor Processing*, 27, 71-78.

Asahi, R., Morikawa, T., Ohwaki, T., Aoki, K., and Taga, Y. (2001). Visible-light photocatalysis in nitrogen-doped titanium oxides. *Science*, *293*(5528), 269-271.

Carp, O., Huisman, C.L., and Reller, A. (2004). Photoinduced reactivity of titanium dioxide. *Progress in Solid State Chemistry*, *32*, 33-177.

Chang, S. M., and Liu, W. S. (2014). The roles of surface-doped metal ions (V, Mn, Fe, Cu, Ce, and W) in the interfacial behavior of TiO_2 photocatalysts. *Applied Catalysis B*: *Environmental*, *156-157*, 466-475.

Chen, L.C., Hsu, C.H., Chan, P.S., Zhang, X., and Huang, C.H. (2014). Improving the performance of dye-sensitized solar cells with TiO_2/graphene/TiO_2 sandwich structure. *Nanoscale Research Letters*, *9*, 380-386

Dong, F., Zhao, W., and Wu, Z. (2008). Characterization and photocatalytic activities of C, N and S Co-doped TiO_2 with 1D nano-structure prepared by the nano-confinement effect. *Nanotechnology*, *19*, 365607-365617.

Galkina, O. L., Sycheva, A., Blagodatskiy, A., Kaptay, G., Katanaev, V. L., Seisenbaeva, G. A., Kessler, V. G., and Agafonov. A.V. (2014). The Sol-gel synthesis of cotton/TiO_2 Composites and their antibacterial properties. *Surface and Coatings Technology*, *253*, 171-179.

Goyal, R. N., Kaur, D. and Pandey, A. K. (2010). Voltammetric sensor based on nano TiO_2 powder modified glassy carbon electrode for determination of dopamine.*The*

Open Chemical and Biomedical Methods Journal, *3*, 115-122.

Joost, U., Juganson, K., Visnapuu, M., Mortimer, M., Kahru, A., Nõmmiste, E., Joost, U., Kisand, V., and Ivask, A. (2015). Photocatalytic antibacterial activity of nano-TiO_2 (anatase)-based thin films: effects on *Escherichia coli* cells and fatty acids. *Journal of Photochemistry and Photobiology B: Biology*, *142*, 178-185.

Kohn, W., and Sham, L. J. (1965). Self-consistent equations including exchange and correlation effects. *Physical Review B, 140*, A1133-A1137.

Liu, B., Wang, X., Cai, G., Wen, L., Song, Y., and Zhao, X. (2009). Low temperature fabrication of V-doped TiO_2 nanoparticles, structure and photo-catalytic studies. *Journal of Hazardous Materials, 169*, 1112-1118.

Mo, S. D. and Ching, W. Y. (1995). Electronic and optical properties of three phases of titanium dioxide: rutile, anatase, and brookite. *Physical Review B, 51*, 13023-13032.

Muctuma, B. K., Shao, G. N., Kim, W. D., and Kim, H. T. (2015). Sol-gel synthesis of mesoporous anatase–brookite and anatase-brookite-rutile TiO_2 nanoparticles and their photocatalytic properties. *Journal of Colloid Interface Science*, *442*, 1-7.

Persson, C., and Ferreira da Silva, A. (2005). Strong polaronic effects on rutile TiO_2 electronic band ddges. *Applied Physics Letter*, *86*, 231912-1 - 231912-3.

Pustelny, T., Procek, M., Maciak, E., Stolarczyk, A., Drewniak, S., Urbańczyk, M., Setkiewicz, M., Gut, K., and Opilski, Z. (2012). Gas sensors based on nano structures of semiconductors ZnO and TiO_2. *Bulletin of the Polish Academy of Sciences Technical Sciences, 60(4), 853-959.*

Rubio-Ponce, A., Conde-Gallardo, A. and Olguín, D. (2008). First-principles study of anatase and rutile TiO_2 doped with Eu ions: a comparison of GGA and LDA+U calculations. *Physical Review B, 78*, 035107-1-035107-8.

Sutrisno, H. (2012). Polymorphic transformation and microstructure characterization of TiO_2 phases prepared by the calcination of hydrogen titanates nanoribbons. *Jurnal Sains* Dasar, *1*(1), 18-32.

Team SCM. (2014). ADF-band version 2014.10, Theoretical Chemistry, Vrije Universiteit, Amsterdam, The Netherlands. http://www.scm.com

Tian, B., Li, C., and Zhang, J. (2012). One step preparation, characterization and visible-light photo-catalytic activity of Cr-doped TiO_2 with anatase and rutile bicrystalline phases. *Chemical Engineering Journal*, *191*, 402-409.

Tian-Hua, X., Chen-Lu, S., Yong, L., and Gao-Rong, H. (2006). Band structures of TiO_2 doped with N, C and B. *Journal of Zhejiang University Science B, 7*(4), 299-303.

Wang, Y., Zhang, R., Li, J., Li., L., and Lin, S. (2014). First-principles study on transition metal-doped anatase TiO_2. *Nanoscale Research Letter, 9*, 46-54.

Xu, T. H., Song C. L., Liu, Y., and Han, G. R., (2006). Band structures of TiO_2 doped with N, C and B. *Journal of Zhejiang University Science B*. 7(4):299-303

Yang, J.H., Bark, C.W., Kim, K.H., and Choi, H.W. (2014). Characteristics of the dye-sensitized solar cells using TiO_2 nanotubes treated with $TiCl_4$. *Materials*, *7*, 3522-3532.

Yang, X., Cao, C., Hohn, K., Erickson, L., Maghirang, R., Hamal, D., and Klabunde, K. (2007). Highly visible light active C- and V-doped TiO_2

for degradation of acetaldehyde. *Journal of Catalysis*, *252*, 296-302.

Zhang, D. R., Liu, H. N., Han, S. Y., Piao, W. X. (2013). Synthesis of Sc- and V-doped TiO_2 nano-particles and photodegradation of rhodamine-B. *Journal of Industrial and Engineering Chemistry*, *19*, 1838-1844.

Zhang, J., Wu, B., Huang, L., Liu, P., Wang, X., Lu, Z., Xu, G., Zhang, E., Wang, H., Kong, Z., Xi, J., and Ji, Z. (2016). Anatase nano-TiO_2 with exposed curved surface for high photocatalytic activity. *Journal of Alloys and Compounds*, *661*, 441-447.

Zhao, K., Wu, Z., Tang, R., and Jiang, Y. (2013). Preparation of highly visible-light photocatalytic active N-doped TiO_2 microcuboids. *Journal of Korean Chemical Society*, *57*(4), 489-492.

Zhao, Y., Qiu, X., and Burda, C. (2008). The effects of sintering on the photocatalytic activity of N-doped TiO_2 nanoparticles. *Chemistry of Material*, *20*, 2629-2636.